

Ionization potentials, electron affinities, and vibrational frequencies of Ge n ($n=5-10$) neutrals and charged ions from density functional theory

Si-Dian Li, Zhi-Gang Zhao, Hai-Shun Wu, and Zhi-Hao Jin

Citation: *The Journal of Chemical Physics* **115**, 9255 (2001); doi: 10.1063/1.1412878

View online: <http://dx.doi.org/10.1063/1.1412878>

View Table of Contents: <http://scitation.aip.org/content/aip/journal/jcp/115/20?ver=pdfcov>

Published by the [AIP Publishing](#)

Articles you may be interested in

Atomic and electronic structures of neutral and charged Pb n clusters ($n = 2 - 15$): Theoretical investigation based on density functional theory

J. Chem. Phys. **126**, 244704 (2007); 10.1063/1.2741537

Assessment of density functional theory optimized basis sets for gradient corrected functionals to transition metal systems: The case of small Ni n ($n \leq 5$) clusters

J. Chem. Phys. **126**, 194102 (2007); 10.1063/1.2735311

Density functional study of the interaction of chlorine atom with small neutral and charged silver clusters

J. Chem. Phys. **122**, 144701 (2005); 10.1063/1.1873612

A density functional study on nitrogen-doped carbon clusters C $_n$ N $_3$ ($n=1-8$)

J. Chem. Phys. **121**, 11661 (2004); 10.1063/1.1814933

Structural and electronic properties of Ge n $m-$ and KGe $n - Zintl$ anions ($n=3-10; m=2-4$) from density functional theory

J. Chem. Phys. **117**, 606 (2002); 10.1063/1.1482068



Ionization potentials, electron affinities, and vibrational frequencies of Ge_n ($n=5-10$) neutrals and charged ions from density functional theory

Si-Dian Li

School of Materials Science and Engineering, Xian Jiaotong University, Xian 710049, People's Republic of China, and Department of Chemistry, Xinzhou Teachers' University, Xinzhou 034000, Shanxi, People's Republic of China

Zhi-Gang Zhao

Department of Chemistry, Xinzhou Teachers' University, Xinzhou 034000, Shanxi, People's Republic of China

Hai-Shun Wu

Institute of Materials Chemistry, Shanxi Normal University, Linfen 041000, Shanxi, People's Republic of China

Zhi-Hao Jin

School of Materials Science and Engineering, Xian Jiaotong University, Xian 710049, People's Republic of China

(Received 24 April 2001; accepted 31 August 2001)

Geometrical and electronic properties of Ge_n ($n=5-10$) neutrals, cations, and anions have been investigated using the density functional method of Becke's three-parameter hybrid functional with the Perdew/Wang 91 expression. Berny structural optimization and frequency analyses are performed with the basis of 6-311G(*d*) for both the neutrals and charged ions. Cohesive energies, ionization potentials, and electron affinities calculated at the optimized ground-state structures agree satisfactorily with recent experimental values. Frequency analyses indicate that the bicapped antitetragonal prism, which was previously proposed as the ground-state structure of Ge_{10}^- , is in fact a first-order stationary point with an imaginary frequency at $95i$ (b_2). The optimized ground-state structure of Ge_{10}^- obtained in this work is a distorted, bicapped antitetragonal prism with the symmetry of C_1 . It is a typical Jahn–Teller distortion. Prominent charge-induced structural changes are also determined for Ge_5^+ , Ge_6^- , Ge_7^+ , Ge_8^+ , Ge_8^- , and Ge_9^- . © 2001 American Institute of Physics. [DOI: 10.1063/1.1412878]

I. INTRODUCTION

Studies on structural and electronic property transitions of semiconductor clusters have received great attention in the past two decades for both fundamental and technological interests.¹⁻¹⁰ Most experimental and electronic structural investigations are focused on Si_n , while much fewer results have been reported for Ge_n , Sn_n , and Pb_n . Mobility measurements by Jarrod *et al.*² and local density approximation calculations by Ho³ and Liu *et al.*⁴ have indicated that small and medium-sized Si_n ($n \leq 27$) exist as prolate stacks of tricapped trigonal prism Si_9 . Germanium and tin clusters are found to follow a very similar growth pattern compared to silicon clusters in small size range, but differ fundamentally in the medium size range.^{5,6} Structural transitions from prolate stacks to the bulk-like spheres occur for Si_n , Ge_n , and Sn_n at different sizes with $n \approx 27$, 65, and 35, respectively. The most accurate theoretical study reported so far on germanium neutrals and anions was performed by Archibong *et al.*⁷ using the B3LYP-DFT and CCSD(T) methods in the range of Ge_2 – Ge_6 . Recent Car–Parrinello molecular dynamics simulated annealing by Lu *et al.*⁸ confirmed again that neutral silicon and germanium clusters follow very similar growth patterns in the size range of $n=2-10$.

The fact that a large portion of experimental results is

obtained from charged particles requires more detailed research on the structural and electronic properties of cations and anions. But, compared to neutrals much fewer strict theoretical calculations for charged clusters have been reported.^{1,4,10} As powerful means in cluster studies, time-of-flight mass spectroscopy, photoelectron spectroscopy (PES), and photoionization threshold measurements all involve the structural and electronic properties of charged clusters. Ionization potentials (I.P.s) of Ge_n ($n=2-57$) featured with the maximum at Ge_{10} were first obtained in recent photoionization threshold measurements by Yoshida *et al.*,⁹ but as far as we know there has been no theoretical calculation reported to reproduce these I.P.s so far. Shvartsburg *et al.*¹⁰ proposed the geometries of Ge_n and Ge_n^+ ($n < 17$) recently using local density approximation (LDA) and the gradient-corrected method, but there were no experimental I.P.s to compare with at that time and frequency analyses were not performed in their calculations. Electron affinities (E.A.s) ($n=1-11$) and HOMO–LUMO gaps ($n=4-32$) of Ge_n have also been bracketed with PES,^{11,12} and again, there have been no adequate theoretical calculations made to explain these results. The main difference between the photoemission spectra of Si_{10}^- and Ge_{10}^- was first explained by Ogut *et al.*¹ utilizing the Langevin molecular dynamics coupled to a simulated anneal-

TABLE I. The optimized ground-state structures, total energies E_t (hartree/particle), the three strongest IR active vibrational frequencies (cm^{-1}) at B3PW91/6-311G(*d*) level, and corresponding 6-311+G(3*df*) energies for Ge_n neutrals, cations, and anions ($n=5-10$).

Cluster	Symmetry	State	6-311G(<i>d</i>)		6-311G(3 <i>df</i>)
			E_t	IR frequency	E_t
Ge_5	D_{3h}	$^1A'_1$	-10 384.991 084	253(e'),219(a''_2),102(e')	-10 385.000 168
Ge_5^+	C_{2v}	2A_1	-10 384.704 235	230(a_1),120(b_1),272(a_1)	-10 384.713 983
Ge_5^-	D_{3h}	$^2A''_2$	-10 385.075 175	251(a''_2),112(e'),213(e')	-10 385.085 979
Ge_6	C_{2v}	1A_1	-12 462.025 730	258(b_1),182(b_2),265(a_1)	-12 462.037 825
Ge_6^+	C_{2v}	2B_1	-12 461.753 461	232(a_1),242(b_1),194(a_1)	-12 461.765 372
Ge_6^-	D_{4h}	$^2A_{2u}$	-12 462.101 395	232(e_u),67(e_u)	-12 462.113 479
Ge_7	D_{5h}	$^1A'_1$	-14 539.059 447	242(e'_1),130(a''_2),126(e'_1)	-14 539.074 019
Ge_7^+	C_{2v}	2A_1	-14 538.780 648	232(b_2),230(a_1),222(b_2)	-14 538.795 416
Ge_7^-	D_{5h}	$^2A''_1$	-14 539.132 156	162(a''_2),227(e'_1),125(a'_2)	-14 539.146 541
Ge_8	C_{2h}	1A_g	-16 616.040 145	290(b_u),213(a_u),200(b_u)	-16 616.056 229
Ge_8^+	C_1	2A	-16 615.789 667	238(a),233(a),221(a)	-16 615.805 612
Ge_8^-	C_1	2A	-16 616.124 612	277(a),112(a),79(a)	-16 616.139 458
Ge_9	C_{2v}	1A_1	-18 693.071 772	277(a_1),265(b_2),225(b_1)	-18 693.089 545
Ge_9^+	C_{2v}	2A_2	-18 692.813 1303	267(a_1),252(b_2),200(b_1)	-18 692.832 471
Ge_9^-	C_1	2A	-18 693.161 9850	234(a),193(a),242(a)	-18 693.177 682
Ge_{10}	C_{3v}	1A_1	-20 770.113 936	240(e),269(a_1),201(a_1)	-20 770.134 925
Ge_{10}^+	C_{3v}	2A_1	-20 769.840 749	233(e),260(a_1),165(a_1)	-20 769.861 800
Ge_{10}^-	C_1	2A	-20 770.193 699	219(a),152(a),127(a)	-20 770.211 799

ing procedure using quantum forces derived from *ab initio* pseudopotentials constructed within the LDA scheme, but more accurate theoretical calculation, frequency analyses, and a stability check are required to confirm this explanation. Following the research of Ge_2 – Ge_6 in Ref. 7, we present in this work a density function theory (DFT) investigation of the geometrical and electronic properties of Ge_n neutrals, cations, and anions in the size range of $n=5-10$ with the Becke's three-parameter hybrid functional with the nonlocal correlation provided by the Perdew/Wang 91 expression (B3PW91). We aim to provide a more comprehensive and reliable database covering the structures, adiabatic and vertical I.P.s and E.A.s, and harmonic vibrational frequencies of Ge_n clusters. We will discuss the charge-induced structural changes of Ge_n in more detail.

II. METHODOLOGY

The B3PW91-DFT/6-311G(*d*) method has been employed to optimize the geometries of Ge_n neutrals and charged ions. Frequency analyses are also performed at the same theoretical level to check whether the optimized structures are transition states or true minima on the potential energy surfaces of corresponding clusters. The choice of density function theory has been fully justified for Ge_n cluster studies due to fact that it is an *ab initio* tool and it includes the electron correlation effect which has been found necessary for germanium clusters at relatively low computational cost.⁷ Electronic properties of these optimized structures including the relative orbital and total energies, I.P.s, and E.A.s are calculated with the same basis sets and compared with corresponding experimental values.^{6,9-12} Electronic property calculation is further performed at the optimized structures with a bigger basis of 6-311G(3*df*). The initial input structures are taken either from published results or arbitrarily constructed and fully optimized via the Berny algorithm.¹³

Symmetry constraints are removed whenever imaginary frequencies are found. For example, the bicapped antitetragonal prism Ge_{10}^- and the adjacent-face bicapped octahedron Ge_8^- labeled as 10(II) and 8(II) in Ref. 1 were found to have imaginary frequencies at $95i$ and $54i$ cm^{-1} , respectively, and the two finally optimized C_1 geometries which have no imaginary frequencies are confirmed to be favored in energies and much lower in symmetries.

All calculations were performed with GAUSSIAN 98 code.¹³ We compared the ground-state structures and electronic states obtained in this work with available results of B3LYP-DFT/6-311+G(3*df*) and CCSD(T) methods by Archibong *et al.* in Ref. 7. The two approaches have produced the same ground-state structures and electronic states in the $n=2-6$ size range, showing the validity of the method employed in this work.

III. RESULTS AND DISCUSSION

Symmetries of the optimized ground-state structures, their total energies, and the three strongest infrared vibrational frequencies are listed in Table I. The ground-state structures obtained for neutrals are identical to those accepted in published references for Si_n and Ge_n .³⁻⁸ The ground-state structures of both cations and anions with $n \geq 7$ are illustrated in Fig. 1. These structures have been confirmed to have no imaginary frequencies and therefore are true minima. For cations and anions (except Ge_6^-), the ground-state structures are either relaxed within the geometries of corresponding neutrals or distorted into new structures with lower energies and much lower symmetries due to Jahn–Teller distortions. For example, the global minimum of Ge_5^+ is a distorted trigonal bipyramid (C_{2v} , 2A_1), which is 0.164 eV lower in energy than trigonal bipyramid Ge_5^+ , while anion Ge_5^- is a relaxed trigonal bipyramid which has

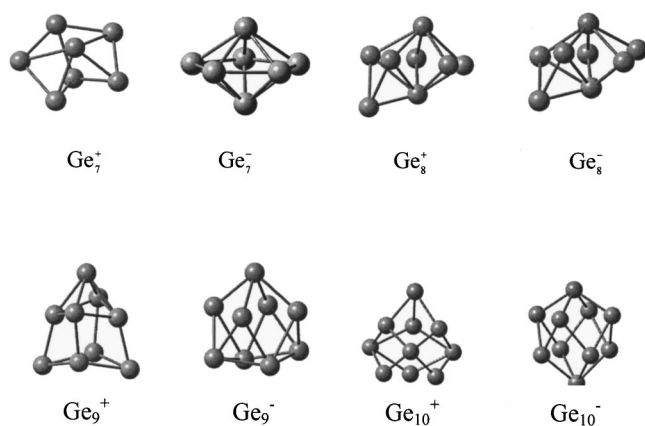


FIG. 1. The ground-state structures of Ge_n cations and anions ($n \geq 7$).

the same symmetry as that of the neutral (D_{3h}). Removing an electron from the edge-capped trigonal bipyramid neutral Ge₆ (C_{2v}) produces a cationic Ge₆⁺ which has the same geometry as the neutral, but adding one electron to neutral Ge₆ results in an octahedron anionic Ge₆⁻ (D_{4h}). The extra electron makes it possible to form four identical bonds around the edge-capping atom in the C_{2v} Ge₆ and transfer the two-fold axis through this atom into a fourfold one. Ge₇⁺ takes a distorted pentagon bipyramid structure (C_{2v}) as its ground-state structure, while Ge₇⁻ is a relaxed pentagonal bipyramid (D_{5h}), the same symmetry as neutral Ge₇. The common feature of the bipyramid Ge₅⁻ (D_{3h}), Ge₆⁻ (D_{4h}), and Ge₇⁻ (D_{5h}) is that the relaxation is the mutual repulsion between the two apex atoms in the vertical direction, while the planar atoms contact inwards. For example, the distances between the two apex atoms in neutral Ge₅, Ge₆, and Ge₇ are 3.12, 2.93, and 2.76 Å, respectively, while in anionic Ge₅⁻, Ge₆⁻, and Ge₇⁻, the corresponding values are 3.63, 3.38, and 3.08 Å. Meanwhile, distances between neighboring atoms in the horizontal planes contract from 3.27, 2.91, and 2.65 Å to 2.93, 2.76, and 2.59 Å, respectively, in these structures. The reason behind this phenomenon is that the LUMOs in the neutrals (A_2'' , A_{2u}'' , and A_2'' for Ge₅, Ge₆, and Ge₇, respectively) have the wave-function character that is centered on the apex atoms. The adjacent-face bicapped octahedron (C_{2v}), which was proposed as the ground-state structure of Ge₈⁻ in Ref. 1, has been confirmed to have an imaginary frequency at $54i \text{ cm}^{-1}$. The lowest-energy structures we found for both Ge₈⁻ and Ge₈⁺ are distorted face-capped pentagonal bipyramid (C_1), which have been confirmed to be lower in energies and have no imaginary frequencies. Structural optimization processes indicate that the tricapped trigonal prism structure, which was proposed as the ground-state structure for Ge₉⁻ in Ref. 1, does not possess the lowest energy. The fully optimized ground-state structure of Ge₉⁻ is a distorted, monocapped antitetragonal prism. This distorted structure is favored in energy and has a much lower symmetry (C_1). It produces a much better adiabatic electron affinity value than all the other structures reported so far. The C_{2v} Bernal structure of Ge₉⁻, which has the same symmetry as Ge₉ neutral, is confirmed to have two imaginary frequencies at $99i$ and $102i \text{ cm}^{-1}$, respectively. Another C_1 symmetry,

which is similar to the neutral in shape and has no imaginary frequencies, has also been obtained for Ge₉⁻. This structure is a local minimum on the potential energy surface of Ge₉⁻, lying 0.89 eV higher in energy than the true ground-state structure discussed above. Our frequency-checked structures for Ge_n⁺ cations are in agreement with that of DFT-LDA and gradient-corrected methods,¹⁰ while structures for Ge_n⁻ anions with $n=8,9$, and 10 have much lower symmetries than that of Ogut *et al.*¹

Ge₁₀⁻ is of special interest in all germanium anions. The bicapped antitetragonal prism structure has been widely accepted as the global minimum for Ge₁₀⁻.^{1,10} To check the stability of this structure, we performed frequency analyses with both B3LYP-DFT/6-311G(*d*) and B3PW91-DFT/6-311G(*d*) methods. It turned out to be a first-order stationary point on the potential energy surface of the anion with an imaginary vibrational frequency at about $95i \text{ cm}^{-1}$ (a b_2 antisymmetrical vibration mode). Very similar results were obtained with the bases of 6-311+G(*d*) and 6-311+G(3*df*), with the latter including diffusion functions for both *d* and *f* orbitals. To find the global minimum, we remove the symmetry constraint and perform a full Berny structural optimization. The lowest-energy structure finally obtained is a distorted, bicapped antitetragonal prism with a much lower symmetry of C_1 . This structure can be derived from C_1 Ge₉⁻ by adding a capping atom (see Fig. 1). It is a typical Jahn–Teller distortion with all the orbital degeneracy released and the total energy lowered, and more importantly, this C_1 structure has no imaginary vibrational frequency. The C_1 geometry is similar to the bicapped antiprism in shape, but different in structural details with the fourfold axis lost, atoms in the two horizontal planes away from positions in perfect planes, the planar atoms unbonded, and the top half a little expanded. Similar to Ge₅⁻, Ge₆⁻, and Ge₇⁻, Ge₁₀⁻ is also expanded in the vertical direction with the distance between the two apex atoms increased from 4.64 Å in the antiprism neutral Ge₁₀ (which has an imaginary frequency at $119i \text{ cm}^{-1}$) to 5.07 Å in the distorted antiprism Ge₁₀⁻. The reason is that the LUMO (a_1) of the neutral antiprism Ge₁₀ has a wave-function character centered at the two symmetrically located apex atoms. Adding an extra electron introduces repulsion force between the two apex atoms and expands the structure in the vertical direction. Meanwhile, the Jahn–Teller effect releases the orbital degeneracy by significantly lowering the molecular symmetry. It is this structural distortion that removes the imaginary harmonic vibration mode ($b_2, 95i \text{ cm}^{-1}$) of the bicapped antiprism structure.

Structural distortion upon charging of germanium clusters is also demonstrated in IR vibrational frequency distributions (see Table I). Ge₁₀⁺ cation exhibits a vibrational spectrum featured with the maximum at $233 \text{ cm}^{-1}(e)$ and the second maximum at $260 \text{ cm}^{-1}(a_1)$, similar but a little redshifted compared to the spectrum of Ge₁₀ neutral. This is because of the fact that both the neutral and cation have the tetracapped trigonal prism C_{3v} structure and the cation is less stable than the neutral because it is lacking one electron. The C_1 distorted bicapped antiprism Ge₁₀⁻ has a very different vibrational spectrum with the three main peaks located at

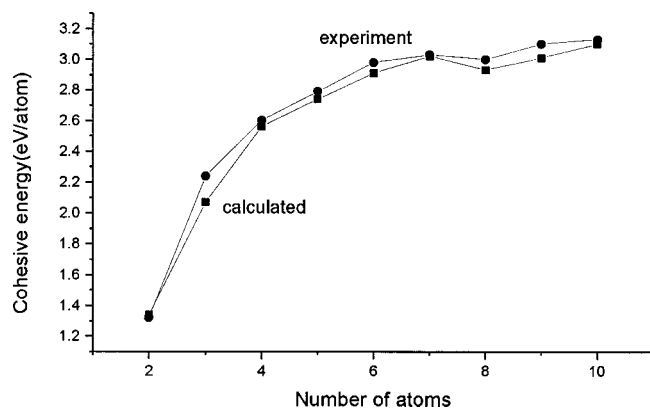


FIG. 2. Comparison between the calculated cohesive energies per-atom (squares) and corresponding experimental values (Refs. 1, 5) (circles) of small germanium clusters.

219(*a*), 152(*a*), and 127(*a*) cm^{-1} and the three weaker peaks situated at 207(*a*), 96(*a*), and 28(*a*) cm^{-1} , respectively. The last peak at 28 cm^{-1} is the lowest vibrational frequency available for this anion cluster. The IR spectrum of $C_1 \text{Ge}_9^-$ differs greatly from those of both $C_{2v} \text{Ge}_9$ and Ge_9^+ because it has a very different structure compared to the neutral and the cation, while for $n=8$, both the C_1 face-capped distorted bipyramid cation and anion vibrate quite differently compared to the C_{2h} neutral. These calculated vibrational frequencies should serve as useful references in distinguishing cluster structures from experimental data in the future.

The calculated cohesive energies (relative to the triplet ground state of Ge atom) agree very satisfactorily with experimental values (see Fig. 2), with Ge_7 as a local maximum, Ge_8 as a local minimum, and Ge_{10} as the most stable species in this size range, in agreement with dissociation and photoionization threshold measurements.^{4,8} Our calculated DFT cohesive energies and corresponding experimental values^{1,5} of Ge_n clusters are 1.34(1.32), 2.07(2.24), 2.56(2.60), 2.74(2.79), 2.91(2.98), 3.02(3.03), 2.93(3.0), 3.01(3.10), and 3.10(3.13) eV for $n=2,3,4,5,6,7,8,9$, and 10, respectively (experimental values are quoted in parentheses). The average discrepancy of calculated cohesive energies relative to available experimental values is less than 3%. This is a much better reproduction of experimental results compared to theoretical results obtained so far using the LDA methods,

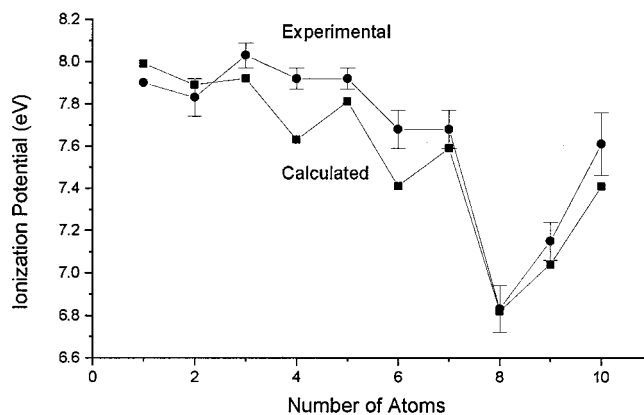


FIG. 3. Comparison between the calculated adiabatic ionization potentials (squares) and corresponding experimental values (circles) of Ge_n ($n=2-10$).

which typically overestimate cohesive energies by about 25%–30%.¹ The special stabilities of Ge_7 and Ge_{10} are in agreement with the fact that medium-sized Ge_n clusters ($n > 10$) dissociate by losing Ge_{10} units in most cases and Ge_7 units in some cases.⁵

The calculated vertical ionization potentials (V.I.P.s), adiabatic ionization potentials (A.I.P.s), adiabatic electron affinities (A.E.A.s), and vertical detachment energies (VDEs) are compared with recent experimental values in Table II, Fig. 3, and Fig. 4. It is believed that if the internal temperature of the neutrals is close to absolute zero and the true threshold is identified, photoionization measurements would provide adiabatic ionization potentials. If the geometry changes significantly upon ionization, the true threshold would probably not be located, and the measured values would lie between A.I.P.s and V.I.P.s.⁴ As can be seen from Fig. 3, our calculated A.I.P.s generally agree well with experimental ionization potentials, reproducing all the variations of the I.P. values observed in experiments,⁹ especially the global minimum at Ge_8 and the obvious recovery at Ge_9 and Ge_{10} . The calculated V.I.P.s are significantly higher than corresponding A.I.P.s and the measured I.P.s lie between the calculated A.I.P.s and V.I.P.s in most cases, relatively closer to A.I.P.s. For $n=4, 5$ and $n=6, 7$, the same I.P. values were bracketed in experiments,⁹ producing the two flat steps in Fig. 3. According to our calculated results, there should be an even–odd alternation with I.P. values in this size range, simi-

TABLE II. Comparison between calculated E.A.s (eV) and I.P.s (eV) with corresponding experimental values.

Ge_n	E.A.s			I.P.s		
	VDE	A.E.A.	Experiment (Refs. 7, 11)	V.I.P.	A.I.P.	Experiment (Ref. 9)
Ge_2	2.67	2.00	2.035(0.001)	8.49	7.89	7.58–7.76
Ge_3	2.51	2.21	2.23(0.01)	8.15	7.92	7.97–8.09
Ge_4	2.02	1.99	1.81(0.09)	7.89	7.63	7.87–7.97
Ge_5	2.98	2.29	2.67(0.17)	8.28	7.81	7.87–7.97
Ge_6	2.67	2.05	2.04(0.08)	7.95	7.41	7.58–7.76
Ge_7	2.31	1.99	1.79(0.06)	8.19	7.59	7.58–7.76
Ge_8	2.80	2.30	2.47(0.11)	7.04	6.82	6.72–6.94
Ge_9	3.30	2.45	2.92(0.11)	7.21	7.04	7.06–7.24
Ge_{10}	3.26	2.17	2.52(0.08)	7.56	7.43	7.46–7.76

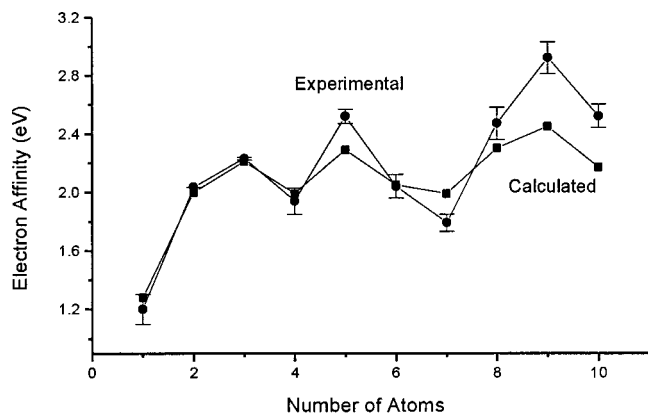


FIG. 4. Comparison between the calculated adiabatic electron affinities (squares) and corresponding experimental values (circles) of Ge_n.

lar to the variation trend of LDA A.I.P. values of silicon clusters.⁴ This prediction needs to be verified in future experiments. Increasing basis sets from 6-311G(*d*) to 6-311G(3*df*) makes no significant improvements to the calculated A.I.P. values. For instance, the 6-311G(*d*) and 6-311G(3*df*) A.I.P. values of Ge_n are 7.63, 7.81, 7.41, 7.59, 6.82, 7.04 and 7.62, 7.79, 7.41, 7.58, 6.82, 7.04 eV for *n* = 4, 5, 6, 7, 8, 9, respectively, indicating that inclusion of more polarization functions in the basis sets produces little help in better reproducing experimental ionization potentials.

As for electron affinities, our calculated A.E.A.s also agree satisfactorily with photoemission experiments (see Fig. 4). The measured maximums at *n* = 3, 5, and 9, the minima at *n* = 4 and 7, and the decreasing at *n* = 10 are all reproduced. The biggest discrepancy (−16%) occurs at *n* = 9, for which the lowest energy structure we found is a distorted tricapped trigonal prism with the symmetry of *C*₁. Another *C*₁ geometry with no imaginary frequencies has also been found for Ge₉[−], but it has a much higher energy. Intensive searches produce no better structures in terms of total energy and electron affinity for Ge₉[−]. As the most stable species in this size range, Ge₁₀ has a high cohesive energy and a high ion-

ization potential, but its electron affinity is low. Table II also lists the vertical detachment energies (VDE) of Ge_n[−] anions, which are generally much higher than both the experimental E.A.s and calculated A.E.A.s.

In summary, we have presented a comprehensive DFT-B3PW91 study for germanium cluster neutrals, cations, and anions in the size range of *n* = 5–10. The DFT cohesive energies, adiabatic ionization potentials, and electron affinities agree well with experiments. Frequency analyses performed at all the optimized geometries have indicated that some of the previously published structures are first-order or second-order stationary points. Prominent charge-induced ground-state structural changes are determined for Ge₅⁺, Ge₆[−], Ge₇⁺, Ge₈⁺, Ge₈[−], Ge₉[−], and Ge₁₀[−]. These results show that Jahn–Teller distortion not only releases the electronic orbital degeneracy but also lowers the symmetries substantially. One should always be cautious to report cluster structures before frequency analyses and stability checks are performed. Even for medium-sized clusters containing less than several tens of atoms, charging of neutral species may still significantly affect the ground-state structures of cations and anions.

¹S. Ogut and J. R. Chelikowsky, Phys. Rev. B **55**, R4914 (1997).

²M. F. Jarrod and V. A. Constant, Phys. Rev. Lett. **67**, 2994 (1992).

³K. M. Ho, A. A. Shvartsburg, B. Pan, Z. Y. Lu, C. Z. Wang, J. G. Wacker, J. L. Fye, and M. F. Jarrod, Nature (London) **392**, 582 (1998).

⁴B. Liu, Z. Y. Lu, B. Pan, C. Z. Wang, and K. M. Ho, J. Chem. Phys. **109**, 9401 (1998).

⁵J. M. Hunter, J. L. Fye, and M. F. Jarrod, Phys. Rev. Lett. **73**, 2063 (1994).

⁶A. A. Shvartsburg and M. F. Jarrod, Chem. Phys. Lett. **317**, 615 (2000).

⁷E. F. Archibong and A. St-Amant, J. Chem. Phys. **109**, 962 (1998).

⁸Z.-Y. Lu, C. Z. Wang, and K. M. Ho, Phys. Rev. B **61**, 2329 (2000).

⁹S. Yoshida and K. Fuke, J. Chem. Phys. **111**, 3880 (1999).

¹⁰A. A. Shvartsburg, B. Liu, Z. Y. Lu, C. Z. Wang, M. F. Jarrod, and K. M. Ho, Phys. Rev. Lett. **83**, 2167 (1999).

¹¹Y. Negishi, H. Kawamata, T. Hayase, M. Gomei, R. Kishi, F. Hayakawa, A. Nakajima, and K. Kaya, Chem. Phys. Lett. **269**, 199 (1997).

¹²Y. Negishi, H. Kawamata, F. Hayakawa, A. Nakajima, and K. Kaya, Chem. Phys. Lett. **294**, 370 (1998).

¹³M. J. Frisch, G. W. Trucks, and H. B. Schlegel *et al.*, GAUSSIAN 98, Revision A.6, Gaussian, Inc., Pittsburgh PA, 1998.